Dyes and Pigments 91 (2011) 269–278

Contents lists available at ScienceDirect

Dyes and Pigments

journal homepage: www.elsevier.com/locate/dyepig

Absorption and fluorescence of soluble polar diketo-pyrrolo-pyrroles

Stanislav Luňák Jr. [a], Martin Vala [b,*], Jan Vyňuchal [a,c,d], Imad Ouzzane [b], Petra Horáková [a], Petra Možíšková [b], Zdeněk Eliáš [a], Martin Weiter [b]

[a] *Faculty of Chemical Technology, University of Pardubice, Studentská 95, CZ-530 09 Pardubice, Czech Republic*
[b] *Faculty of Chemistry, Centre for Materials Research, Brno University of Technology, Purkyňova 464/118, CZ-612 00 Brno, Czech Republic*
[c] *Research Institute of Organic Syntheses, Rybitví 296, CZ-533 54 Rybitví, Czech Republic*
[d] *Synthesia a.s., Pardubice, Semtín 103, CZ-532 17 Pardubice, Czech Republic*

ARTICLE INFO

Article history:
Received 26 October 2010
Received in revised form
29 April 2011
Accepted 4 May 2011
Available online 19 May 2011

Keywords:
Diketo-pyrrolo-pyrrole
Fluorescence
Solvatochromism
Solid-state fluorescence
Twisted intramolecular charge transfer
Organic electronics

ABSTRACT

Six soluble derivatives of 3,6-diphenyl-2,5-dihydro-pyrrolo[3,4-*c*]pyrrole-1,4-dione *N*-alkylated on pyrrolinone ring with polar substituents in *para* positions of pendant phenyl rings were synthesized; five of them are reported for the first time. Absorption and fluorescence spectra were studied in solvents of different polarity. The compounds show small solvatochromism of absorption and a moderate positive solvatochromism of fluorescence, especially when substituted by strong electron-donating piperidino substituent. A significant decrease of fluorescence quantum yields and its biexponential decay for dipolar derivatives in polar solvents was tentatively ascribed to the formation of twisted intramolecular charge transfer (TICT) excited state. All six compounds show fluorescence in polycrystalline solid-state with the maxima covering a range over 200 nm in visible and near infrared region.

1. Introduction

Although originally developed as high performance organic pigments [1,2,3], various structural modifications made diketo-pyrrolo-pyrroles (DPPs) interesting as advanced materials for modern optical and electronic technologies. The devices based on DPPs copolymerized with e.g. carbazoles [4] and especially with oligothiophenes [5,6] reached the promising efficiencies as organic field-effect transistors (OFET) [5] and bulk heterojunction (BHJ) photovoltaic solar cells (OPV) [4,6]. Aside from DPP copolymers, which form rather specific area with dramatically increasing number of references, DPP monomers have been recently found also to be perspective in photovoltaics, either in the BHJ OPV [7], or in dye-sensitized solar cells (DSSC) [8] type. The common structural features of DPP derivatives designed for these purposes are: The substituted (usually alkylated, in some cases acylated [9]) pyrrolinone nitrogens, changing the insoluble pigments to molecules enabling wet solution based processing, and the presence of electron-donating groups as a counterpart to diketo-pyrrolo-pyrrole core with an electron-accepting character.

We have recently published the syntheses and spectral properties of parent DPP chromophore 3,6-diphenyl-2,5-dihydro-pyrrolo[3,4-*c*]pyrrole-1,4-dione (**I**) and its electron-donor (piperidino) and electron-acceptor (cyano) symmetrically and unsymmetrically substituted derivatives (**II**–**VI**, Fig. 1) [10]. The derivatives have shown bathochromic and hyperchromic shift of absorption and bathofluoric shift of fluorescence with respect to parent compound **I** invoked above all by piperidino electron-donating substituent. Dimethyl sulfoxide (DMSO) was found to be the only common solvent able to dissolve all these pigments. In order to make these compounds better treatable we have decided to substitute them on pyrrolinone nitrogens and so eliminate the intermolecular hydrogen bonding [1]. On the contrary to more usual *N*-alkylation by alkylhalogen, used in our previous studies [11,12], we applied ethyl bromoacetate in this case (Fig. 1). Such substitution was reported only once resulting in compound **VII** with highly distorted structure in crystal according to X-ray diffraction [13] giving thus a good chance to be highly soluble because of the absence of $\pi-\pi$ stacking, another insolubility implicating phenomenon aside from CO–NH hydrogen bonding [14]. Compounds **VIII**–**XII** were never reported, thus they are fully characterized in Experimental. This is the first case, to the best of our knowledge, when simple push-pull substituted well soluble DPP derivative (**XII**) is studied.

---

* Corresponding author. Tel.: +420 541 149 411; fax: +420 541 149 398.
E-mail address: vala@fch.vutbr.cz (M. Vala).

0143-7208/$ – see front matter © 2011 Elsevier Ltd. All rights reserved.
doi:10.1016/j.dyepig.2011.05.004

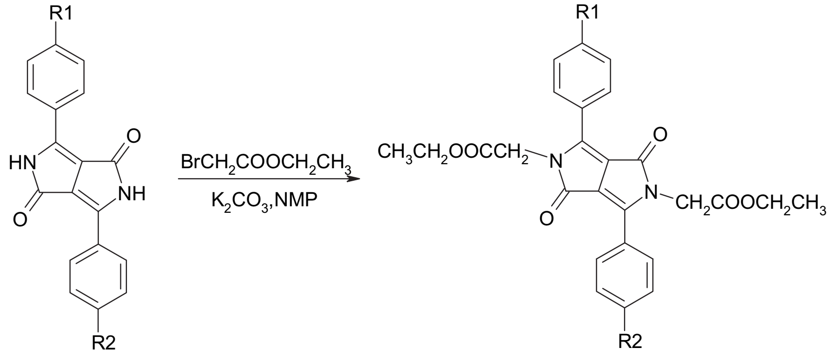

Symbol	R_1	R_2
I	H	H
II	CN	H
III	CN	CN
IV	H	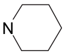
V	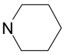	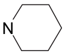
VI	CN	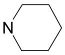

Symbol	R_1	R_2
VII	H	H
VIII	CN	H
IX	CN	CN
X	H	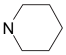
XI	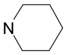	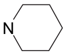
XII	CN	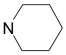

Fig. 1. General synthetic route and notation of the compounds under study.

DPP derivatives are known for a long time to be strongly fluorescent in solution [15]. The only reported exceptions to the best of our knowledge are the compounds, in which the pyrrolinone carbonyl group underwent a nucleophilic substitution by heteroarylacetonitrile [16] or bis(trimethylsilyl)carbodiimide [17] forming the products loosing the true DPP character. The aim of this study was thus first to investigate in detail the dependence of absorption and fluorescence spectra and fluorescence efficiencies in solution on the character of pendant phenyl substitution in **VIII**–**XII** with respect to on-phenyl unsubstituted **VII** and *N*-unsubstituted precursors **I**–**VI**. Contrary to hardly soluble pigments **I**–**VI**, it was possible also to measure a solvatochromism on **VII**–**XII**, which was never studied in detail before.

As we observed the luminescence of some of these *N,N′*-dialkylated DPPs in solid-state just by naked eye during the samples handling (opposite to totally non-luminescent precursors **I**–**VI**), we studied also this not particularly common behaviour but being of growing interest [18,19,20]. Since the pioneering work of Langhals [21], the solid-state fluorescence of several DPP derivatives was mentioned in literature [9,22,23], but the full understanding of this phenomenon requires more systematic studies on the representative series of derivatives.

2. Experimental

2.1. Syntheses and analyses

The synthesis of the starting derivatives **I**–**VI** was described in Ref. [10]. Compound **VII** was synthesized from compound **I** in a similar way as described earlier and confirmed by melting point 210–212 °C (lit. [13]. 207–208 °C). *N*-methyl-2-pyrrolidone (NMP), ethyl bromoacetate and potassium carbonate were purchased from Sigma-Aldrich, so as the three solvents used in the spectral studies.

*2.1.1. Preparation of diethyl-3-(phenyl)-6-(4-cyanophenyl)-2,5-dihydropyrrolo[3,4-c]pyrrole-1,4-dione-diacetate (**VIII**)*

Compound **II** (8 g, 0.0256 mol), potassium carbonate (35.4 g, 0.256 mol) and NMP (480 ml) were charged to a three-necked flask. Reaction mixture was heated to 120 °C. Ethyl bromoacetate (42.8 g, 0.256 mol) in NMP (185 ml) was added to the reactor dropwise during 40 min. Then the reaction was stirred and heated to 120 °C for 2 h. After cooling, the reaction was slowly poured onto ice-cold water (1400 ml). The obtained precipitate was filtered off and washed with water until neutral washings. The crude product was recrystallized from a mixture of methanol and water (2:1). Yield: 2.02 g (16.29%) of compound **VIII**. m.p. 139–141 °C.

Calculated: C (66.90), H (4.78), N (8.66), Found: C (66.84), H (4.73), N (8.46)

MW = 485 Da; Positive-ion APCI-MS: m/z 486 $[M + H]^+$, (100%)

^{1}H chemical shifts: 8.12 (2H, m, Ar*H*); 7.99 (2H, m, Ar*H*); 7.84 (2H, m, Ar*H*); 7.66 (3H, m, Ar*H*); 4.64 (2H, s, $-NCH_2$,); 4.63 (2H, s, $-NCH_2$,); 4.115 (2H, q, $J = 7.1$ Hz, $-OCH_2$); 4.110 (2H, q, $J = 7.1$ Hz, $-OCH_2$); 1.142 (3H, t, $J = 7.1$ Hz, $-CH_2CH_3$); 1.140 (3H, t, $J = 7.1$ Hz, $-CH_2CH_3$)

^{13}C chemical shifts: 168.37 (1C, $>C{=}O$); 168.29 (1C, $>C{=}O$); 161.30 (1C, $>C{=}O$); 161.03 (1C, $>C{=}O$); 149.52 (1C, Ar*C*); 145.37 (1C, Ar*C*); 133.02 (2C, Ar*C*); 132.09 (1C, Ar*C*); 131.33 (1C, Ar*C*); 129.26 (2C, Ar*C*); 129.21 (2C, Ar*C*); 128.68 (2C, Ar*C*); 126.88 (1C, Ar*C*); 118.26 (1C, $-C{\equiv}N$); 113.52 (1C, Ar*C*); 109.90 (1C, Ar*C*); 108.47

(1C, ArC); 61.41 (1C, $\mathrm{N}{-}CH_2$); 61.38 (1C, $\mathrm{N}{-}CH_2$); 43.38 (1C, $-\mathrm{O}CH_2$); 43.26 (1C, $-\mathrm{O}CH_2$); 13.92 (2C, $-\mathrm{CH_2}CH_3$)

2.1.2. *Preparation of diethyl-3,6-di-(4-cyanophenyl)-2,5-dihydropyrrolo[3,4-c]pyrrole-1,4-dione-diacetate (**IX**)*

Compound **III** (5 g, 0.0148 mol), potassium carbonate (20.42 g, 0.148 mol) and NMP (272 ml) were charged into a three-necked flask. Reaction mixture was heated to 120 °C and ethyl bromoacetate (24.7 g, 0.148 mol) in NMP (116 ml) was added dropwise to the reactor during 40 min. Then the reaction was stirred and heated to 120 °C for 2 h. After cooling, the reaction was slowly poured onto ice-cold water (760 ml). The obtained precipitate was filtered off and washed with water until neutral washings. The crude product was recrystallized from methanol. Yield: 0.81 g (10.7%) of orange compound **IX**, m.p. 177–179 °C.

Calculated: C (68.49), H (6.12), N (7.73), Found: C (68.49), H (6.04), N (7.63)

^{1}H chemical shifts: 8.14 (4H, m, ArH); 8.01 (4H, m, ArH); 4.64 (4H, s, $-\mathrm{N}CH_2$); 4.10 (4H, q, $J = 7.1$ Hz, $-\mathrm{O}CH_2$); 1.13 (6H, t, $J = 7.1$ Hz, $-\mathrm{CH_2}CH_3$)

^{13}C chemical shifts: 168.23 (2C, $>C{=}\mathrm{O}$); 160.97 (2C, $>C{=}\mathrm{O}$); 146.92 (2C, ArC); 133.05 (4C, ArC); 131.06 (2C, ArC); 129.33 (4C, ArC); 118.36 (2C, $-C{\equiv}\mathrm{N}$); 113.82 (2C, ArC); 109.82 (2C, ArC); 61.45 (2C, $\mathrm{N}{-}CH_2$); 43.40 (2C, $-\mathrm{O}CH_2$); 13.90 (2C, $-\mathrm{CH_2}CH_3$)

2.1.3. *Preparation of diethyl-3-(phenyl)-6-(4-piperidinophenyl)-2,5-dihydropyrrolo[3,4-c]pyrrole-1,4-dione-diacetate (**X**)*

Dry and pure NMP (150 ml), compound **IV** (3.7 g, 0.01 mol) and potassium carbonate (15.2 g, 0.11 mol) were charged to a three-necked flask. Reaction mixture was heated to 120 °C. Ethyl bromoacetate (18.4 g, 0.11 mol) in NMP (80 ml) was added dropwise to the reactor during 40 min. Then the reaction mixture was stirred and heated to 120 °C for 2 h. After cooling, the reaction was slowly poured onto ice-cold water (500 ml). The obtained precipitate was filtered off and washed with water until neutral washings. The crude product was recrystallized from methanol. Yield: 3.2 g (59%) of compound **X**, m.p. 207–214 °C.

Calculated: C (65.88), H (4.34), N (10.97), Found: C (65.47), H (4.44), N (10.82)

MW = 510 Da; Positive-ion APCI-MS: m/z 511 $[\mathrm{M + H}]^+$ (100%)

^{1}H chemical shifts: 7.83 (2H, m, ArH); 7.78 (2H, m, ArH); 7.61 (3H, m, ArH); 7.1 (2H, m, ArH); 4.66 (2H, s, $-\mathrm{N}CH_2$); 4.61 (2H, s, $-\mathrm{N}CH_2$); 4.17 (2H, q, $J = 7.1$ Hz, $-\mathrm{O}CH_2$); 4.12 (2H, q, $J = 7.1$ Hz, $-\mathrm{O}CH_2$); 3.48 (4H, m, $-\mathrm{CH_2CH_2}CH_2\mathrm{N}$); 1.64 (6H, m, $-CH_2\mathrm{CH_2CH_2N}$ and $-\mathrm{CH_2}CH_2\mathrm{CH_2N}$); 1.19 (6H, t, $J = 7.1$ Hz, $-\mathrm{CH_2}CH_3$); 1.15 (6H, t, $J = 7.1$ Hz, $-\mathrm{CH_2}CH_3$)

^{13}C chemical shifts: 168.65 (1C, $>C{=}\mathrm{O}$); 168.61 (1C, $>C{=}\mathrm{O}$); 161.99 (1C, $>C{=}\mathrm{O}$); 161.06 (1C, $>C{=}\mathrm{O}$); 152.74 (1C, ArC); 149.20 (1C, ArC); 144.33 (1C, ArC); 131.05 (1C, ArC); 130.70 (2C, ArC); 129.03 (2C, ArC); 128.45 (2C, ArC); 127.59 (1C, ArC); 114.51 (1C, ArC); 113.47 (2C, ArC); 108.75 (1C, ArC); 105.91 (1C, ArC); 61.29 (1C, $\mathrm{N}{-}CH_2$); 61.21 (1C, $\mathrm{N}{-}CH_2$); 47.69 (2C, $-\mathrm{CH_2CH_2}CH_2\mathrm{N}$); 43.88 (1C, $-\mathrm{O}CH_2$); 43.34 (1C, $-\mathrm{O}CH_2$); 25.00 (2C, $-\mathrm{CH_2}CH_2\mathrm{CH_2N}$); 24.07 (1C, $-CH_2\mathrm{CH_2CH_2N}$); 14.02 (1C, $-\mathrm{CH_2}CH_3$); 13.97 (1C, $-\mathrm{CH_2}CH_3$)

2.1.4. *Preparation of diethyl-3,6-di-(4-piperidinophenyl)-2,5-dihydropyrrolo[3,4-c]pyrrole-1,4-dione-diacetate (**XI**)*

Compound **V** (5 g, 0.011 mol), potassium carbonate (15.2 g, 0.11 mol) and NMP (205 ml) were charged into three-necked flask. Reaction mixture was heated to 120 °C and ethyl bromoacetate (18.38 g, 0.11 mol) in NMP (80 ml) was added dropwise to the reactor during 40 min. Then the reaction was stirred and heated to 120 °C for 2 h. After cooling, the reaction was slowly poured onto ice-cold water (600 ml). The obtained precipitate was filtered off and washed with water until neutral washings. The crude product was recrystallized from methanol. Yield: 3.57 g (54.3%) compound **XI**, m.p. 213–217 °C.

Calculated: C (68.99), H (6.75), N (8.94), Found: C (68.80), H (6.85), N (8.78)

MW = 626 Da; Positive-ion APCI-MS: m/z 627 $[\mathrm{M + H}]^+$ (100%)

^{1}H chemical shifts: 7.75 (4H, m, ArH); 7.01 (4H, m, ArH); 4.64 (4H, s, $-\mathrm{N}CH_2$); 4.16 (4H, q, $J = 7.2$ Hz, $-\mathrm{O}CH_2$); 3.41 (8H, m, $-\mathrm{CH_2CH_2}CH_2\mathrm{N}$); 1.64 (12H, m, $-CH_2\mathrm{CH_2CH_2N}$ and $-\mathrm{CH_2}CH_2\mathrm{CH_2N}$); 1.18 (6H, t, $J = 7.2$ Hz, $-\mathrm{CH_2}CH_3$)

^{13}C chemical shifts: 130.27 (4C, ArC); 113.67 (4C, ArC); 61.19 (2C, $\mathrm{N}{-}CH_2$); 47.83 (4C, $-\mathrm{CH_2CH_2}CH_2\mathrm{N}$); 43.80 (2C, $-\mathrm{O}CH_2$); 24.97 (4C, $-\mathrm{CH_2}CH_2\mathrm{CH_2N}$); 14.04 (2C, $-\mathrm{CH_2}CH_3$); Remaining signals were not detected due to low solubility of the sample.

2.1.5. *Preparation of diethyl-3-(4-cyanophenyl)-6-(4-piperidinophenyl)-2,5-dihydropyrrolo[3,4-c]pyrrole-1,4-dione-diacetate (**XII**)*

Compound **VI** (3 g, 0.0076 mol), potassium carbonate (10.5 g, 0.076 mol) and NMP (140 ml) were charged into three-necked flask (500 ml). Reaction mixture was heated to 120 °C and ethyl bromoacetate (14 g, 0.082 mol) in NMP (60 ml) was added dropwise to the reactor during 40 min. Then the reaction was stirred and heated to 120 °C for 2 h. After cooling, the reaction was slowly poured onto ice-cold water (400 ml). The obtained precipitate was filtered off and washed with water until neutral washings. The crude product was recrystallized from the mixture of n-hexan and methanol (7:3). Yield: 2.26 g (70.4%) of compound **XII**, m.p. 192–195 °C.

Calculated: C (67.59), H (5.67), N (9.85), Found: C (67.40), H (5.72), N (9.65)

MW = 568 Da; Positive-ion APCI-MS: m/z 569 $[\mathrm{M + H}]^+$ (100%)

^{1}H chemical shifts: 8.08 (2H, m, ArH); 8.01 (2H, m, ArH); 7.87 (2H, m, ArH); 7.10 (2H, m, ArH); 4.69 (2H, s, $-\mathrm{N}CH_2$); 4.65 (2H, s, $-\mathrm{N}CH_2$); 4.17 (2H, q, $J = 7.0$ Hz, $-\mathrm{O}CH_2$); 4.11 (2H, q, $J = 7.1$ Hz, $-\mathrm{O}CH_2$); 3.50 (4H, s, $-\mathrm{CH_2CH_2}CH_2\mathrm{N}$); 1.65 (6H, s, $-CH_2\mathrm{CH_2CH_2N}$ and $-\mathrm{CH_2}CH_2\mathrm{CH_2N}$); 1.19 (3H, t, $J = 7.1$ Hz, $-\mathrm{CH_2}CH_3$); 1.15 (3H, t, $J = 7.0$ Hz, $-\mathrm{CH_2}CH_3$)

^{13}C chemical shifts: 168.62 (1C, $>C{=}\mathrm{O}$); 168.57 (1C, $>C{=}\mathrm{O}$); 162.07 (1C, $>C{=}\mathrm{O}$); 160.80 (1C, $>C{=}\mathrm{O}$); 152.95 (1C, ArC); 150.68 (1C, ArC); 141.33 (1C, ArC); 132.92 (2C, ArC); 131.85 (1C, ArC); 131.07 (2C, ArC); 129.04 (2C, ArC); 118.44 (1C, $-C{\equiv}\mathrm{N}$); 114.04 (1C, ArC); 113.36 (2C, ArC); 112.73 (1C, ArC); 110.35 (1C, ArC); 105.81 (1C, ArC); 61.39 (1C, $\mathrm{N}{-}CH_2$); 61.32 (1C, $\mathrm{N}{-}CH_2$); 47.63 (2C, $-\mathrm{CH_2CH_2}CH_2\mathrm{N}$); 44.05 (1C, $-\mathrm{O}CH_2$); 43.37 (1C, $-\mathrm{O}CH_2$); 25.05 (2C, $-\mathrm{CH_2}CH_2\mathrm{CH_2N}$); 24.10 (1C, $-CH_2\mathrm{CH_2CH_2N}$); 14.04 (1C, $-\mathrm{CH_2}CH_3$); 13.97 (1C, $-\mathrm{CH_2}CH_3$)

2.2. *Structure and purity characterization*

2.2.1. *Mass spectrometry*

The ion trap mass spectrometer MSD TRAP XCT Plus system (Agilent Technologies, USA) equipped with APCI probe was used. Positive-ion and negative-ion APCI mass spectra were measured in the mass range of 50–1000 Da in all the experiments. The ion trap analyzer was tuned to obtain the optimum response in the range of the expected m/z values (the target mass was set from m/z 289 to m/z 454). The other APCI ion source parameters: drying gas flow rate 7 $\mathrm{dm^3\ min^{-1}}$, nebulizer gas pressure 60 psi, drying gas temperature 350 °C, nebulizer gas temperature 350 °C. The samples were dissolved in a mixture of DMSO/acetonitrile and methanol in various ratios. All the samples were analyzed by means of direct infusion into LC/MS.

2.2.2. *Elemental analysis*

Perkin-Elmer PE 2400 SERIES II CHNS/O and EA 1108 FISONS instruments were used for elemental analyses.

2.2.3. Nuclear magnetic resonance

Bruker AVANCE 500 NMR spectrometer operating at 500.13 MHz for ^{1}H was used for measurements of the ^{1}H NMR spectra. The compounds were dissolved in hexadeuteriodimethyl sulfoxide used as deutered standard. The ^{1}H chemical shifts were referred to the central signal of the solvent ($\delta = 2.55$).

2.3. Optical characterization

2.3.1. UV–VIS absorption and fluorescence spectroscopy

The referred UV–VIS absorption spectra in solution were recorded using Varian Carry 50 UV–VIS spectrometer. The fluorescence spectra in solution were measured in 90° configuration at Aminco Bowmann S2 fluorimeter. The solid-state luminescence spectra were recorded on Perkin-Elmer LS 55 equipped with an accessory for solid-state measurements from the same producer. Polycrystalline samples were placed under quartz plate and the emission spectra were recorded using front face geometry.

2.3.2. Fluorescence quantum yields

The fluorescence quantum yields (φ_F) in solution were calculated according to the comparative method [24], where for each test sample gradient of integrated fluorescence intensity versus absorbance $F = f(A)$ is used to calculate the φ_F using two known standards. The standards were previously cross-calibrated to verify the method. This calibration revealed accuracy about 5%. As the reference we used Rhodamine B and Rhodamine 6G with φ_{Fl} 0.49 [25] and 0.950 ± 0.005 [26], respectively. The excitation wavelength was chosen to be the same as for the laser excited experiments i.e. 532 nm. Since the **VII** has very low absorption coefficient at this exciting wavelength, we used Fluorescein (0.91 ± 0.02) [20] and Coumarin 6 (0.78) [27] because of the better spectral overlap. The excitation wavelength in this case was 460 nm.

2.3.3. Fluorescence lifetimes

The fluorescence lifetime τ_F was measured using Andor Shamrock SR-303i spectrograph and Andor iStar ICCD camera. The samples were excited by third harmonic of EKSPLA PG400 Nd:YAG laser (355 nm) with light pulse time duration of ~30 ps. The temporal resolution of the system is approximately 25 ps. In order to avoid chromatic aberrations, the emitted light from the sample was collected by two off-axis mirrors.

2.4. Computational procedures

All theoretical calculations for compounds **VII**–**XII** were carried out on exactly same level as for previously reported precursors **I**–**VI** [10], in order to be directly comparable. The ground state (S_0) geometry was optimized using quantum chemical calculations based on DFT. Hybrid three-parameter B3LYP functional in combination with 6-311G(d,p) basis was used. No constraints were preliminary employed, but, as the nonconstrainted computations converged to symmetrical structures for compounds **VII**, **IX** and **XI**, the final computations were carried out with C_i symmetry constraint. No imaginary frequencies were found by vibrational analysis, confirming that the computed geometries were real minima on the ground state hypersurfaces.

TD DFT computations of the vertical excitation energies were carried out on the computed S_0 geometries. The same exchange-correlation functional (B3LYP) was used in TD DFT calculations with rather broader basis set (6-311+G(2d,p)). Solvent effect of DMSO was involved by non-equilibrium PCM.

All methods were taken from Gaussian09W program suite [28], and the default values of computational parameters were used. The results were analyzed using GaussViewW from Gaussian Inc, too.

3. Results and discussion

3.1. Syntheses

Although looking quite simple (Fig. 1), *N,N*-dialkylation of DPPs is a two-step process complicated by extremely low solubility of starting pigments, which sometimes leads to the presence of mono-alkylated intermediate in reaction mixture, even if an excess of both alkylating agent and HBr neutralizing potassium carbonate is used [11]. In-depth study of this reaction was recently carried out [29]. The reports on the syntheses targeted directly on *N*-mono-alkylated DPPs are relatively rare, but there was recently shown, that these compounds can be highly sensitive and selective fluorescent sensors for fluoride anions [30]. All six DPP derivatives **VII**–**XII** in the presented study were prepared with moderate to high yields and the special purification procedures like chromatography or fractional crystallization were not necessary in order to obtain the product of the desired quality. We ascribe this fact to higher reactivity of bromine on ethyl bromoacetate as compared to e.g. *n*-butyl bromide. The compounds show good solubility over a wide range of solvents, so we have carried out the spectral measurements in highly polar DMSO, in order to have direct comparison with our previous results obtained for *N*-non-alkylated pigment precursors **I**–**VI** [10] or *N*-butylated analogues of **VII** and **XI** [11,12], in acetonitrile, as a representative of less polar solvents, and in almost non-polar but easily polarizable toluene.

3.2. DFT computed structure

As expected, DFT optimized geometries of **VII**–**XII** predict non-zero dihedral angles, describing phenyl-pyrrolinone rotation (Table 1), on the contrary to strictly planar precursors **I**–**VI** [10]. The computed values of dihedral angles are the result of a compromise between sterical effect of methylene and *ortho* phenyl hydrogens (more or less the same for all six derivatives), invoking nonplanarity, and conjugation effect (dependent primarily on *para* phenyl substituent of each derivative), maximal for planar arrangement. The effect of the substituent on opposite pendant phenyl is marginal (less than 1°). Average values are thus 26°, 36° and 38° for piperidino, cyano and unsubstituted phenyls, respectively.

As these dihedral angles are crucial for the interpretation of absorption spectra, they should be verified by comparison with the experiment. The only known X-ray diffraction structure of compound **VII** [13] is a bit problematic from this point of view. The molecule is highly unsymmetrical in crystal with $\alpha = 36.5°$, i.e. quite close to the computed value 38.2°, and $\beta = 68.8°$, i.e. totally out of a reasonable agreement. These results show a dramatic role of packing forces in DPP crystal. As discussed earlier [31], there are always some perturbation of planarity even for theoretically planar DPP pigments, bearing evidence of relatively flat minima of ground state geometry with respect to phenyl-pyrrolinone rotation. One can expect, that the equilibrium between sterical and conjugation

Table 1
DFT computed phenyl–pyrrolinone dihedral angles and PCM (DMSO) TD DFT computed excitation energies converted to wavelengths.

Compound	α [°]	β [°]	λ_{00} [nm]	f_{osc}
VII	38.2	38.2	465	0.512
VIII	34.7	38.2	495	0.563
IX	36.3	36.3	509	0.615
X	38.0	26.1	518	0.835
XI	26.6	26.6	546	1.138
XII	35.2	25.5	561	0.923

α [°] = R_1-phenyl-pyrrolinone dihedral angle; β [°] = R_2-phenyl-pyrrolinone dihedral angle; λ_{00} [nm] = theoretical excitation energy; f_{osc} = oscillator strength.

effects may be even more fragile for *N*-alkylated derivatives and thus the effect of packing forces may be more dramatic. That is probably the case of the X-ray structure of **VII**. Unfortunately, such distorted molecular structure can give only limited evidence on the accuracy of the computed structures. We have tested the relevance of DFT method to predict the dihedral angles of *N,N*-disubstituted compound **I** on another two known X-ray structures, in which C_i molecular symmetry in crystal is retained. The results were quite encouraging. The computed value for *N,N*-dimethyl **I** (30.3°) matches well the experimental one (30.4° [32]), and an agreement for *N,N*-diallyl **I** (theor. 31.2°, exp. 35.8° [13]) is also acceptable. There are no X-ray data for *N,N*-di-*n*-butyl **I** available, but a lot of them exist, for its derivatives (see bellow), so we computed also the dihedral angle for this compound. Its value (26.4°) is considerably lower, than for compound **VII** (38.2°).

We searched the Cambridge structural database (CSD) using *ConQuest* procedure [33] in order to find the structures similar to the derivatives **VII**–**XII**. There were found four files with X-ray structures of DPP derivatives with both pyrrolinone nitrogen substituted by *n*-butyl and at least one pendant phenyl either unsubstituted, or substituted with amino or cyano groups in *para* position: KAKMAL ($R_1 = $ CN, $R_2 = $ H, $\alpha = 45.2°$, $\beta = 32.6°$) [34], XATKIN ($R_1 = R_2 = $ CN, $\alpha = \beta = 43.1°$), NAWREJ ($R_1 = $ H, $R_2 = $ diphenylamino, $\alpha = 32.8°$, $\beta = 30.5°$) and XATKEJ ($R_1 = $ H, $R_2 = $ 4-MeO-phenyl, $\alpha = 41.0°$, $\beta = 42.3°$) [35]. Another relevant data come from recently published *N,N*-dibenzylated DPPs. Such group recall probably similar steric hindrance with respect to phenyl, as dihedral angles of chlorinated derivative ($R_1 = R_2 = $ Cl, $\alpha = 41.6°$, $\beta = 43.9°$) [23] are very similar to *N,N*-dibutylated dibromo derivative found in CSD in XATJAE file ($R_1 = R_2 = $ Br, $\alpha = \beta = 45.0°$) [35]. So the results for *N,N*-dibenzylated dimorfolino derivative ($R_1 = R_2 = $ morfolino, $\alpha = \beta = 28.1°$) [23] are close to those obtained for diphenylamino substituent (file NAWREJ) in accordance with an interpretation based of a mixing of two resonance structures for dimorfolino (and generally diamino) DPP derivatives [23].

Finally, DFT predicted decrease of the phenyl-pyrrolinone dihedral angle accompanying *p*-piperidino substitution is in accordance with the relevant experimental data, at least qualitatively. On the other hand, small lowering of this dihedral angle connected with *p*-cyano substituent is inconsistent not only with the data coming from both above mentioned *p*-cyano substituted derivatives, but even with a general trend represented by other electron-accepting substituents, i.e. halogens.

In order to test the sensitivity of dihedral angles of CN substituted derivatives on a quantum chemical method, we carried out the calculations on Hartree–Fock (HF) level with the same 6-311G(d,p) basis set. We obtained the dihedral angles considerably higher ($\alpha = 52.4°$, $\beta = 52.1°$ for **VIII**, $\alpha = \beta = 52.4°$ for **IX** and, $\alpha = 52.5°$, $\beta = 47.9°$ for **XII**) compared to those ones coming from DFT calculations (Table 1). But these computations also do not considerably distinguish 4–CN–phenyl-pyrrolinone and phenyl-pyrrolinone dihedral angles.

3.3. Absorption and fluorescence spectra in DMSO

The absorption maxima of **VII**–**XII** in DMSO show hypsochromic and hypochromic shifts (Table 2a, Fig. 2) with respect to corresponding precursors **I**–**VI** [10]. Hypsochromic shift is in fact a net effect of three contributions: 1) An increase of excitation energy due the less efficient conjugation because of the loss of molecular planartity, 2) the redistribution of the intensities of vibronic sub-bands from 0–0 maximum of **I**–**VI** in favour of 0–1 in **VII**–**XII**, as shown by a successive *N*-alkylation of **I** and **V** [11,12] and 3) the opposite effect – the decrease of excitation energy due to the increase of electron-donating strength of a pyrrolinone nitrogens in central DPP core composed of two coupled merocyanines (H-chromophore). We consider that the second and third contributions are almost constant over the whole series and the differences in hypsochromic shifts caused by *N*-alkylation go almost exclusively on account of the first one, i.e. the substituent dependent changes in the ground state planarity.

Table 2
The spectroscopic properties of **VII**–**XII** in a) DMSO, b) acetonitrile and c) toluene.

Compound	λ_A (nm)	ε (λ_A) (l mol^{-1} cm^{-1})	λ_F(nm)	φ_F	$\Delta\lambda_{Stokes}$ (cm^{-1})	τ_F (ns)
a) DMSO						
VII	460	15,800	519	0.56	2470	7.34 ± 0.08
VIII	471	16,000	547	0.51	2950	7.07 ± 0.03
IX	480	13,300	557	0.72	2880	6.50 ± 0.04
X	516	32,200	601	0.12	2740	1.17 ± 0.02
						6.7 ± 1.2
XI	540	45,100	603	0.45	1940	3.45 ± 0.02
XII	541	42,300	654	<0.01	3190	0.217 ± 0.002
						3.72 ± 0.10
b) Acetonitrile						
VII	454	19,200	512	0.31	2490	6.70 ± 0.04
VIII	464	16,900	538	0.75	2960	5.78 ± 0.03
IX	473	19,400	549	0.32	2930	6.67 ± 0.04
X	500	35,400	587	0.01	2960	1.12 ± 0.01
						2.70 ± 0.20
XI	523	50,500	590	0.20	2170	3.70 ± 0.03
XII	524	34,800	638	<0.01	3410	<0.10
						3.57 ± 0.02
c) Toluene						
VII	462	18,500	520	0.36	2410	5.93 ± 0.04
VIII	472	22,570	544	0.43	2800	4.24 ± 0.02
IX	482	17,700	558	0.29	2830	6.48 ± 0.04
X	499	35,000	563	0.34	2280	4.00 ± 0.02
XI	520	44,400	575	0.38	1840	3.20 ± 0.02
XII	527	36,500	603	0.16	2390	4.41 ± 0.05

λ_A – the position of the absorption maximum; ε – molar absorption coefficient at the λ_A; λ_F – the position of the fluorescence maximum; φ_F – the fluorescence quantum yield; $\Delta\lambda_{Stokes}$ – the Stokes shift (λ_F–λ_A); τ_F – the observed fluorescence lifetime.

The highest hypsochromic shift with respect to non-alkylated precursor was found for di-cyano substituted **IX** (59 nm), mono-cyano substituted **VIII** (53 nm) and rather lower for unsubstituted **VII** (45 nm). On the other hand the lowest hypsochromic shift was observed for di- and mono-piperidino substituted **XI** (20 nm) and **X** (24 nm), while the shift of unsymmetrical compound **XII** (35 nm) with both types of substituents lies between the symmetrically

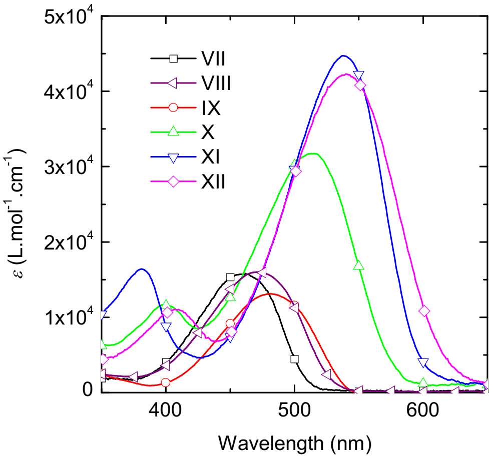

Fig. 2. Molar absorption coefficients of the studied DPP derivatives in DMSO.

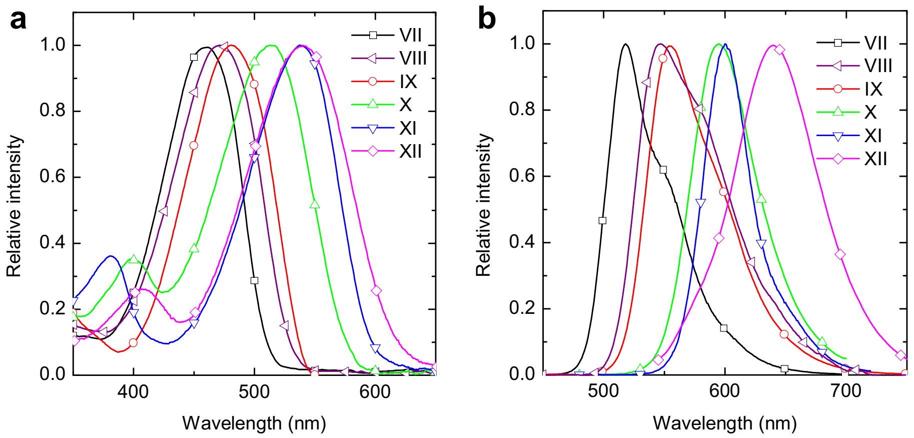

Fig. 3. Normalized absorption (a) and fluorescence (b) spectra of **VII**–**XII** in DMSO.

substituted **IX** and **XI**. Although solute–solvent interaction may play some role, we relate this behaviour mainly to the dependence of the dihedral angle describing the phenyl-pyrrolinone rotation on a nature of *para* substituent of this pendant phenyl. The conclusion is thus clear: piperidino substitution dramatically decreases the phenyl-pyrrolinone dihedral angles in accordance with DFT predictions, while cyano substitution increases these angles considerably, contrary to theory.

PCM TD DFT computed data relate to the experimental maxima only qualitatively. More precisely, the series can be divided into two groups of derivatives. The first one (**VII**, **X** and **XI**) show the deviation between computed λ_{00} (Table 1) and experimental λ_A (Table 2a) 2–6 nm, while the difference for cyano substituted derivatives is significantly bigger (20–22 nm for mono-cyano substituted **VIII** and **XII** and even 29 nm for di-cyano **IX**). As there were no such discrepancies between theory and experiment for planar derivatives **I**–**VI** [10], we ascribe this inconsistency also to underestimated dihedral angles in DFT calculated geometries.

Finally, the suspicion revealed in part 3.2. filled up and the absorption spectra clearly show, that the dihedral angle between *p*-cyano-phenyl and pyrrolinone rings should be relatively higher than for unsubsubstituted phenyl-pyrrolinone case, contrary for the DFT prediction. PCM (DMSO) TD DFT 6-311 + G(2d,p) calculations carried out on the above mentioned more distorted HF geometry resulted in a considerable blue shift ($\lambda_{00} = 426$.nm for **VIII**, 435 nm for **IX** and 477 nm for **XII**), compared the values obtained on DFT geometry (Table 1), i.e. the values of λ_{00} are in this case much lower compared to the experimental λ_A (Table 2a) showing an evidence on nonrealistic distortion coming from HF geometries.

The hypsochromic shift of **VII** with respect to *N*,*N*-dibutylated **I** (7 nm) [12] and opposite bathochromic shift of **XI** with respect to *N*,*N*-dibutylated **V** (−4 nm) [12] do not support, that $-CH_2COOCH_2CH_3$ grouping is sterically significantly more efficient than $-CH_2CH_2CH_2CH_3$ as it would relate to the computed difference of phenyl rotation in **VII** (38.2°) and *N*,*N*-dibutylated **I** (26.4°). The absorption spectra do not corfirm that unsymmetrical highly distorted X-ray structure of **VII** [13] is retained in solution.

The relation between fluorescence maxima of corresponding members of *N*-alkylated and non-alkylated sets is different from absorption and much less clear on the first view (Table 2a, Fig. 3). The maxima of unsubstituted **I** with respect to **VII** are almost the same (+2 nm on behalf of **VII**), while **IX** shows hypsofluoric shift with respect to **III** (−8 nm). The fluorescence maximum of compound **VIII** shows also a hypsofluoric shift with respect to **II** (−3 nm, i.e. *exactly* between +2 nm and −8 nm for symmetrical pairs **I**/**VII** and **III**/**IX**). *N*,*N*-dialkylated electron-donor substituted derivatives **X** (+14 nm) and **XI** (+15 nm) show moderate bathofluoric shifts as compared to **IV** and **V**, respectively. Push-pull derivative **XII** shows almost identical maximum as **VI** (the difference is +1 nm), i.e. its value lies between **III**/**IX** and **V**/**XI** pairs as in absorption. As a consequence the Stokes shift of compound **XII** is absolutely the highest one (3190 cm^{-1}), i.e. significantly higher than for non-alkylated compound **VI** (2060 cm^{-1}). An increment of a Stokes shift increase connected with *N*,*N*-disubstitution is relatively similar (1090–1270 cm^{-1}) for all three pairs of piperidino substituted compounds and rather higher (1930–2070 cm^{-1}) for unsubstituted or only cyano substituted pairs.

The main reason for the general increase of the Stokes shift due to *N*-alkylation is caused by the fact, that it is considered as a difference between absorption and fluorescence maxima. The maxima correspond to 0–0 vibronic transition in fluorescence spectra for all twelve compounds, to 0–0 vibronic transition in absorption for **I**–**VI** [10] and to 0–1 transition for **VII**–**XII** (Fig. 3). An increase of Stokes shift caused by a redistribution of vibronic bands intensities in absorption may not be strictly constant, but probably quite similar for all six pairs. The rest of the changes in Stokes shift goes on account of the differences in internal (geometrical) and external (solvent) relaxation, when going from vertical Franck-Condon (FC) state to relaxed excited state. Internal relaxation is probably mainly connected with the changes of above discussed dihedral angles. In order to have a better view on external contribution, it was necessary to carry out the spectral measurements in other solvents with different (lower) polarity.

3.4. Solvatochromism

It was impossible to measure the absorption and fluorescence solvatochromism of **I**–**VI** because of their insolubility in other than highly polar solvents able to form H-complexes with solute. The spectral data for *N*-alkylated derivatives in toluene and acetonitrile are summarized in Table 2b, c and the spectra are shown on Figs. 4 and 5. The shape of the absorption spectra is the same in all three solvents, i.e. the vibronic structure is completely unresolved even in toluene, while the vibronic structure of fluorescence spectra is best resolved for all compounds in toluene, in which clearly 0–0 vibronic transition is the absolute maximum, and its resolution decreases in acetonitrile and is almost lost in DMSO.

Compound **VII** shows small negative solvatochromism, when going from toluene to acetonitrile (−8 nm) and almost the same positive shift from acetonitrile to DMSO (+6 nm). The shifts of its fluorescence maxima are almost identical, thus Stokes shift is the

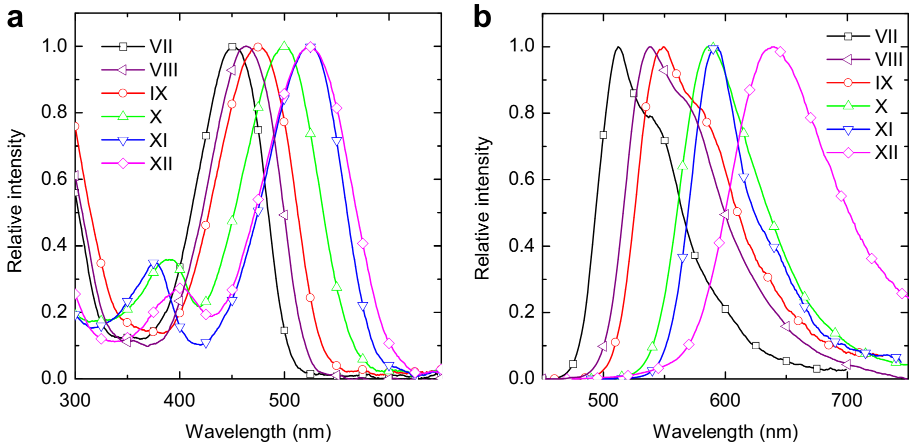

Fig. 4. Normalized absorption (a) and fluorescence (b) spectra in acetonitrile.

same in all three solvents. The solvent induced shifts of **IX** are nearly the same within 1 nm. The spectral shifts when going from toluene to acetonitrile markedly evoke the situation found for BODIPY dyes [36] and the interpretation is the same. While the absorption maximum of their hybrid **VIII** lies exactly between **VII** and **IX** in all solvents, the fluorescence maximum is generally closer to **IX** and a small growth of Stokes shift with solvent polarity from toluene (2800 cm^{-1}) to acetonitrile (2960 cm^{-1}) is observed. Thus **VIII** is only a bit more polar in relaxed than in FC excited state.

The introduction of piperidino group brings two general trends with respect to excited state relaxation in compounds **X**–**XII**: The contribution of internal relaxation is decreased, which well relates with lower rotation of *p*-piperidino-phenyl in FC state, while the external contribution is increased, as the electron-donating substitution changes the intramolecular charge distribution. The former statement can be documented by lower Stokes shift of **XI** (1840 cm^{-1}) with respect to **VII** (2410 cm^{-1}) in non-polar toluene. The latter sentence is generally proved by a dependence of Stokes shift on a solvent polarity, i.e. its increase is less than 160 cm^{-1} for **VII**–**IX** and notably higher for **XI** (330 cm^{-1}), **X** (680 cm^{-1}) and especially **XII** (1020 cm^{-1}) when going from toluene to acetonitrile. Thus, the largest observed Stokes shift of **XII** (3190 cm^{-1} in DMSO) is in fact mainly done by donor-acceptor substitution (2060 cm^{-1} in DMSO for **VI** [10]) and the additional effect of *N*-alkylation goes mainly on account of a redistribution of vibronic intensities in absorption spectrum of **XII**.

The solvent induced shifts in absorption of **X**–**XII** are less than 4 nm when going from toluene to acetonitrile, reflecting very similar polarity of the ground and excited FC states. Positive solvatochromism of fluorescence is moderate: 15 nm for symmetrical **XI**, and 24 and 35 nm for asymmetrical **IX** and **XII**, respectively, that can be ascribed to relaxed excited state solvent stabilization. The positive solvatochromism in absorption of **X**–**XII** when going from acetonitrile to DMSO is almost constant (16–17 nm), very similar to the corresponding shift in fluorescence (13–16 nm) and a bit higher than for **VII**–**IX** (6–7 nm in absorption and 7–9 nm in fluorescence). It means, that further increase of solvent polarity does not lead to additional excited state relaxation and the energy of the excited FC and relaxed states is lower only because the excited state charge distribution interacts more favourably than the ground state itself with the reaction field of more polar solvent (induced by ground state distribution) [37].

The highest solvent induced rise of Stokes shift, i.e. for compound **XII** between toluene and acetonitrile (+1020 cm^{-1}), is significantly lower than for 4-(dimethylamino)-4′-cyano-1,4-diphenylbutadiene (**DCB**, +4640 cm^{-1} between n-hexane and acetonitrile [38]), in which only central 1,4-diphenyl-butadiene backbone of **XII** is push-pull substituted. This difference goes exclusively on account of much lower value of positive fluorescence solvatochromism of compound **XII** (+35 nm) with respect to **DCB** (+129 nm), while the solvatochromism of absorption is almost the same (−3 nm for **XII** and +2 nm for **DCB**), i.e. negligible between above mentioned

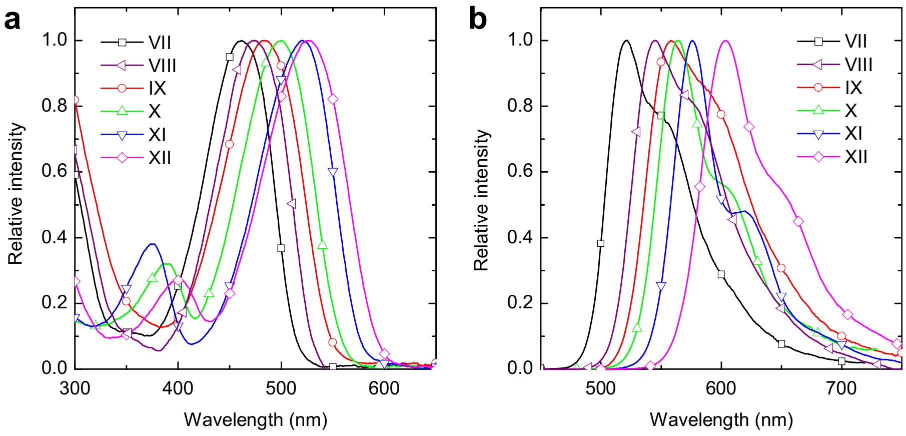

Fig. 5. Normalized absorption (a) and fluorescence (b) spectra in toluene.

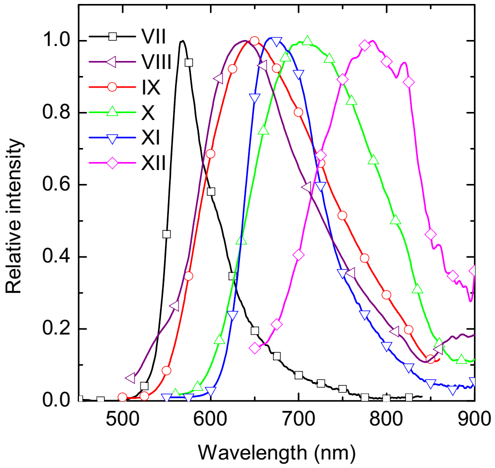

Fig. 6. Solid-state fluorescence spectra of DPP derivatives.

non-polar and polar solvents. Thus, although compounds **X** and **XII** behave qualitatively like push-pull like chromophores, quantitatively their fluorescence solvatochromism is quite limited.

Compound **XI** is formally a quadrupolar molecule with D-π-A-π-D character. Such compounds may or may not undergo an excited state symmetry-breaking in highly polar solvents [39]. The shifts of absorption (3 nm) and fluorescence (15 nm) maxima of **XI**, when going from toluene to acetonitrile, is relatively small (although not as small as for e.g. squaraines [39]), indicating very small (if any) excited state perturbation. Compound **XI** is thus an intermediate quadrupolar chromophor with expected high two-photon absorption cross-section. Their relatively high values estimated for *N*-octylated *p*-diphenylamino substituted DPPs confirm this idea [40].

3.5. *Photophysical behaviour*

Fluorescence quantum yields (φ_F) and lifetimes (τ_F) for **VII**–**XII** in all three solvents are summarized in Table 2. Corresponding photophysical data for non-alkylated precursors **I** ($\varphi_F = 0.74$, $\tau_F = 6.21$ ns) and **V** ($\varphi_F = 0.58$, $\tau_F = 3.66$ ns) in DMSO were reported previously [12] and we now supply them by φ_F and τ_F for further two piperidino substituted precursors **IV** ($\varphi_F = 0.48$, $\tau_F = 3.49$ ns) and **VI** ($\varphi_F = 0.14$, $\tau_F = 3.90$ ns) also in DMSO and not published in Ref. [10]. Both these compounds show monoexponential fluorescence decay.

All six compounds **VII**–**XII** also show a relatively high φ_F in toluene and the fluorescence decay is strictly monoexponential with lifetimes similar to corresponding non-alkylated precursors in DMSO. However, there is a dramatic change for compounds **X** and **XII** when going to polar solvents. The quantum yields of fluorescence are significantly decreased, especially for **XII** (Table 2b, c), and the decay is biexponential. It implies, that some specific process connected with the excited state intramolecular charge transfer (ICT) must be present. Such behaviour may be connected with a conformational change in excited state known as twisted intramolecular charge transfer (TICT). 4-piperidino-benzonitrile is known to undergo such process even more willingly than 4-dimethylamino-benzonitrile, a prototype molecule with respect to TICT [41]. Nevertheless, it is generally very difficult to prove this idea, if not supported by two emission bands in steady-state fluorescence. According to our opinion, the observable fluorescence of **XII** in polar solvents comes from the minor portion of excited molecules, for which the charge separating twist did not pass. Nevertheless this explanation is only speculative and the final solution of this problem would require further sophisticated photophysical experiments that are out of the scope of this article.

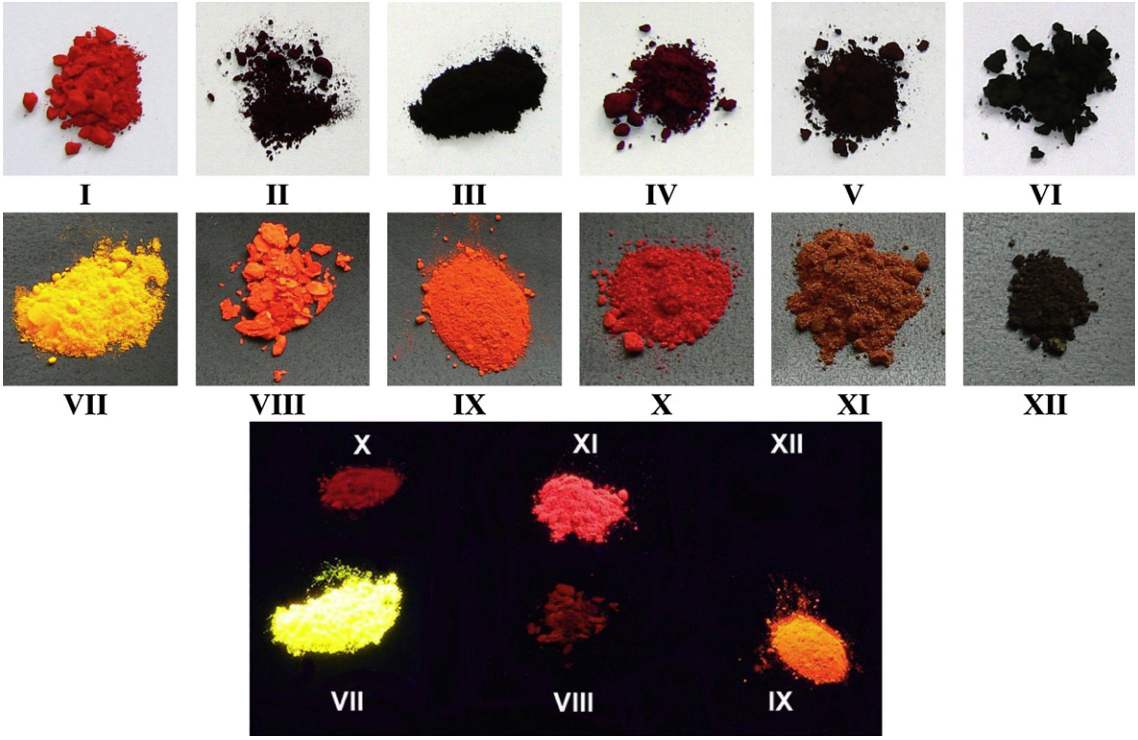

Fig. 7. Polycrystalline samples of **I**–**XII** under daylight (top) and fluorescence of the samples of **VII**–**XII** under UV irradiation (365 nm) with the same settings of Panasonic DMC-FZ7 camera (bottom).

3.6. Solid-state fluorescence

All six studied DPP derivatives show pronounced solid-state fluorescence, on the contrary to any of their non-alkylated precursors **I**–**VI**. The spectra are shown on Fig. 6. The fluorescence of symmetrical **VII**, **IX** and **XI** is strong, easily observable by naked eye under UV irradiation (Fig. 7). The fluorescence of unsymmetrical **VIII** and **X** is less intense, but observable. Solid-state fluorescence of push-pull derivative **XII** is almost not observable (and totally undetectable by a camera – Fig. 7) partly because of its significantly lower intensity and also as it falls almost fully into the infrared region. The values of emission maxima in polycrystalline phase are 568 nm (**VII**), 639 nm (**VIII**), 648 nm (**IX**), 708 nm (**X**), 670 nm (**XI**) and 784 nm (**XII**), and hence, their sequence corresponds to that one in polar solvent (Table 2a) except the changeover of **X** and **XI** pair. The corresponding changeover of dipolar **VIII** and formally quadrupolar **IX** did nor occur, but the fluorescence maximum of hybrid **VIII** in solid state is significantly closer to parent **IX** than to **VII**. The spectral maxima are shifted bathochromically with respect to even the most polar solvent (DMSO). The smallest shift was found for compound **VII** (49 nm) without any polar substituent, the moderate one for centrosymmetric compounds **XI** (67 nm) and **IX** (91 nm), and the highest one for polar **VIII** (92 nm) and **X** (107 nm) and, especially, for push-pull substituted **XII** (130 nm).

Although the intermolecular interactions in highly organized crystal phase cannot be in principle described by simple solute–solvent terminology, the red shifts probably predicate about the polarity inside the crystal environment, i.e. 1) it is effectively more polar than DMSO in all cases and 2) the highest effect is of course in crystals composed from the molecules with non-zero dipole moment. The changeover of solid-state fluorescence maxima of **X** and **XI** is thus a logical continuation of the trend observed in solvents with increasing polarity (Table 2a–c). Although the crystal of **XII** has evidently more polar environment than in DMSO solution, the fluorescence of **XII** does not definitely diminishes in it. We consider this phenomenon as further support of TICT role in the deactivation cascade of **XII** in DMSO, while the excited state twisting is disabled in rigid crystal environment. Almost identical behaviour and interpretation was reported for push-pull substituted 1,6-diphenyl-1,3,5-hexatriene [42].

Generally, the solid-state fluorescence of organic pigments is considered as a property of individual molecule conserved in crystal phase [43]. In other words, the quenching process connected with electron-phonon coupling in crystals of **I**–**VI**, eliminated by *N,N*-dialkylation in their derivatives **VII**–**XII**, relate very probably to impossibility of $\pi-\pi$ stacking in crystal [21]. Such disabled stacking may come either from intramolecular sterical hindrance, i.e. molecular nonplanarity, or the intermolecular one, e.g. disabled proximity of molecular planes due to large volume side chains. We consider the former contribution as crucial in this case.

4. Conclusions

Six *N*-alkylated soluble DPP derivatives with polar substituents in *para* positions of pendant phenyls were synthesized, in order to make original non-alkylated pigment precursors better treatable. The compounds are non-planar with phenyl rings rotated out of diketo-pyrrolo-pyrrole plane. The degree of this rotation is decreased by the electron-donating substituents, while increased by the electron-withdrawing substituents, contrary to the DFT predictions. The compounds show small solvatochromism of absorption and a moderate positive solvatochromism of fluorescence, if substituted by strong electron-donating substituent. The significant decrease of fluorescence quantum yields and its biexponential decay for dipolar derivatives in polar solvents was tentatively ascribed to the formation of non-fluorescent TICT excited state. All compounds show fluorescence in polycrystalline solid-state with the maxima covering a range over 200 nm in visible and near infrared region, where the solid-state fluorescence is quite rare [18].

Acknowledgement

The research was supported by the Academy of Sciences of the Czech Republic via project KAN401770651, by the Ministry of Industry and Trade of the Czech Republic via 2A-1TP1/041 project, by the Czech Science Foundation via P205/10/2280 project and by the project “Centre for Materials Research at FCH BUT” No. CZ.1.05/2.1.00/01.0012 from ERDF.

References

[1] Iqbal A, Jost M, Kirchmayer R, Pfenninger J, Rochat AC, Wallquist O. Synthesis and properties of 1,4-diketopyrrolo[3,4-c]pyrroles. Bulletin des Societes Chimiques Belges 1988;97(8–9):615–43.
[2] Wallquist O. Diketopyrrolopyrrole (DPP) pigments. In: Smith HM, editor. High performance pigments. Weinheim: Wiley-VCH; 2002. p. 159–84.
[3] Herbst M, Hunger K. Industrial organic pigments. Weinheim: Wiley-VCH; 2004. pp. 487–494.
[4] Aïch RB, Zou Y, Leclerc M, Tao Y. Solvent effect and device optimization of diketopyrrolopyrrole and carbazole copolymer based solar cells. Org Electron 2010;11(6):1053–8.
[5] Bürgi L, Turbiez M, Pfeiffer R, Bienewald F, Kirner HJ, Winnewisser C. High-mobility ambipolar near-infrared light-emitting polymer field-effect transistors. Adv Mater 2008;20(11):2217–24.
[6] Bijleveld JC, Zoombelt AP, Mathijssen SGJ, Wienk MM, Turbiez M, De Leeuw DM, et al. Poly(diketopyrrolopyrroleterthiophene) for ambipolar logic and photovoltaics. J Am Chem Soc 2009;131(46):16616–7.
[7] Walker B, Tamayo AB, Dang XD, Zalar P, Seo JH, Garcia A, et al. Nanoscale phase separation and high photovoltaic efficiency in solution-processed, small-molecule bulk heterojunction solar cells. Adv Funct Mater 2009;19(19):3063–9.
[8] Qu S, Wu W, Hua J, Kong C, Long Y, Tian H. New diketopyrrolopyrrole (DPP) dyes for efficient dye-sensitized solar cells. J Phys Chem C 2010;114(2):1343–9.
[9] Tamayo AB, Walker B, Nguyen TQ. A low band gap, solution processable oligothiophene with a diketopyrrolopyrrole core for use in organic solar cells. J Phys Chem C 2008;112(30):11545–51.
[10] Luňák Jr S, Vyňuchal J, Vala M, Havel L, Hrdina R. The synthesis, absorption and fluorescence of polar diketo-pyrrolo-pyroles. Dyes Pigm 2009;82(2):102–8.
[11] Vala M, Weiter M, Vyňuchal J, Toman P, Luňák Jr S. Comparative studies of diphenyl-diketo-pyrrolopyrrole derivatives for electroluminescence applications. J Fluoresc 2008;18(6):1181–6.
[12] Vala M, Vyňuchal J, Toman P, Weiter M, Luňák Jr S. Novel, soluble diphenyl-diketo-pyrrolopyrroles: experimental and theoretical study. Dyes Pigm 2010;84(2):176–82.
[13] Colonna G, Pilati T, Rusconi F, Zecchi G. Synthesis and properties of some new N, N′-disubstituted 2,5-dihydro-1,4-dioxo-3,6-diphenylpyrrolo[3,4-c]pyrroles. Dyes Pigm 2007;75(1):125–9.
[14] Thetford D, Cherryman J, Chorlton AP, Docherty R. Theoretical molecular modelling calculations on the solid state structure of some organic pigments. Dyes Pigm 2004;63(3):259–76.
[15] Potrawa T, Langhals H. Fluorescent dyes with large stokes shifts-soluble dihydropyrrolopyrrolediones. Chem Ber 1987;120(7):1075–8.
[16] Fischer GM, Ehlers AP, Zumbusch A, Daltrozzo E. Near-infrared dyes and fluorophores based on diketopyrrolopyrroles. Angew Chem Int Ed 2007;46(4):3750–3.
[17] Imoda T, Mizuguchi J. Strikingly different luminescent properties arising from single crystals grown from solution or from the vapor phase in a diketo-pyrrolo-pyrrole analog. J Appl Phys 2007;102(7):073529(1)–073529(7).
[18] Park SY, Kubota Y, Funabiki K, Shiro M, Matsui M. Near-infrared solid-state fluorescent naphtooxazine dyes attached with bulky dibutylamino and perfluoroalkenyloxy groups at 6- and 9-positions. Tetrahedron Lett 2009;50(10):1131–5.
[19] Matsui M, Ikeda R, Kubota Y, Funabiki K. Red solid-state fluorescent aminoperfluorophenazines. Tetrahedron Lett 2009;50(35):5047–9.
[20] Park SY, Ebihara M, Kubota Y, Funabiki K, Matsui M. The relationship between solid-state fluorescence intensity and molecular packing of coumarin dyes. Dyes Pigm 2009;82(3):258–67.
[21] Langhals H, Potrawa T, Nöth H, Linti G. The influence of packing effects on the solid-state fluorescence of diketopyrrolopyrroles. Angew Chem Int Ed 1989;28(4):478–80.

[22] Tamayo AB, Tantiwiwat M, Walker B, Nguyen TQ. Design, syntheses, and self-assembly of oligothiophene derivatives with a diketopyrrolopyrrole core. J Phys Chem C 2008;112(39):15543–52.
[23] Kuwabara J, Yamagata T, Kanbara T. Solid-state structure and optical properties of highly fluorescent diketopyrrolopyrrole derivatives synthesized by cross-coupling reaction. Tetrahedron 2010;66(21):3736–41.
[24] Williams ATR, Winfield SA, Miller JN. Relative fluorescence quantum yields using a computer-controlled luminescence spectrometer. Analyst (Cambridge, United Kingdom) 1983;108(1290):1067–71.
[25] Casey KG, Quitevis EL. Effect of solvent polarity on nonradiative processes in xanthene dyes: rhodamine B in normal alcohols. J Phys Chem 1988;92(23):6590–4.
[26] Magde D, Wong R, Seybold PG. Fluorescence quantum yields and their relation to lifetimes of rhodamine 6G and fluorescein in nine solvents: improved absolute standards for quantum yields. Photochem Photobiol 2002;75(4):327–34.
[27] Reynolds GA, Drexhage KH. New coumarin dyes with rigidized structure for flashlamp-pumped dye lasers. Opt Commun 1975;13:222–5.
[28] Gaussian 09, Revision A.1, Frisch MJ, Trucks GW, Schlegel HB, Scuseria GE, Robb MA, Cheeseman JR, et al., 2009.
[29] Stas S, Sergeyev S, Geerts Y. Synthesis of diketopyrrolopyrrole (DPP) derivatives compridsing bithiophene moieties. Tetrahedron 2010;66(10):1837–45.
[30] Qu Y, Hua J, Tian H. Colorimetric and ratiometric red fluorescent chemosensor for fluoride ion based on diketopyrrolopyrrole. Org Lett 2010;12(15):3320–3.
[31] Luňák Jr S, Vyňuchal J, Hrdina R. Geometry and absorption of diketo-pyrrolo-pyrrole isomers and their π-isoelectronic furo-furanone analogues. J Mol Struct 2009;919(1–3):239–45.
[32] Mizuguchi J, Grubenmann A, Wooden G, Rihs G. Structures of 3,6-diphenylpyrrolo[3,4-c]pyrrole-1,4-dione and 2,5-dimethyl-3,6-diphenylpyrrolo[3,4-c]pyrrole-1,4-dione. Acta Crystallogr B 1992;48(5):696–700 (The value in the text was taken from file KUHKUT in CSD).
[33] Bruno IJ, Cole JC, Edgington PR, Kessler M, Macrae CF, McCabe P, et al. New software for searching the Cambridge Structural Database and visualizing crystal structures. Acta Crystallogr B 2002;58(3–1):389–97.
[34] File KAKMAL cited in CSD as: Poppe M, Gompper R, Polborn K. 2005, Private Communication.
[35] Files XATKIN, NAWREJ, XATKEJ and XATJAE cited in CSD as: Ostermann D, Gompper R, Polborn K. 2005, Private Communication.
[36] Qin W, Rohand T, Baruah M, Stefan A, Van der Auweraer M, Dehaen W, et al. Solvent-dependent photophysical properties of borondipyrromethene dyes in solution. Chem Phys Lett 2006;420(4–6):562–8.
[37] Zoon PD, Brouwer AM. A push-pull aromatic chromophore with a touch of merocyanine. Photochem Photobiol Sci 2009;8(3):345–53.
[38] El-Gezawy H, Rettig W, Lapouyade R. Solvatochromic behaviour of donor-acceptor-polyenes: dimethylamino-cyano-diphenylbutadiene. J Phys Chem A 2006;110(1):67–75.
[39] Terenziani F, Painelli A, Katan C, Charlot M, Blanchard-Desce M. Charge instability in quadrupolar chromophores: symmetry breaking and solvatochromism. J Am Chem Soc 2006;128(49):15742–55.
[40] Guo EQ, Ren PH, Zhang YL, Zhang HC, Yang WJ. Diphenylamine end-capped 1,4-diketo-3,6-diphenylpyrrolo[3,4-c]pyrrole (DPP) derivatives with large two-photon absorption cross-sections and strong two-photon excitation red fluorescence. Chem Commun 2009;39:5859–61.
[41] Grabowski ZR, Rotkiewicz K, Rettig W. Structural changes accompanying intramolecular electron transfer: focus on twisted intramolecular charge-transfer states and structures. Chem. Rev. 2003;103(10):3899–4031.
[42] Sonoda Y, Goto M, Tsuzuki S, Tamaoki N. Fluorescence spectroscopic properties and crystal structure of a series of donor–acceptor diphenylpolyenes. J Phys Chem A 2006;110(50):13379–87.
[43] Plötner J, Dreuw A. Solid state fluorescence of pigment yellow 101 and derivatives: a conserved property of the individual molecules. Phys Chem Chem Phys 2006;8(10):1197–204.